ELectronics EXpress

LETTER

IEICE Electronics Express, Vol.10, No.24, 1–8

Design and simulation of a high isolation RF MEMS shunt capacitive switch for C-K band

Yasser Mafinejad[1a)], **Majid Zarghami**[2], **Abbas Z. Kouzani**[1], **and Khalil Mafinezhad**[2]

[1] *School of Engineering, Deakin University, Waurn Ponds, Victoria 3216, Australia*

[2] *MEMS and RF MEMS Research Group, School of Electrical and Computer Engineering, Sadjad Institute of Higher Education, Razavi Khorasan, Mashhad, Iran*

a) *ymafinej@deakin.edu.au*

Abstract: This paper presents a wide band RF MEMS capacitive switch. The LC resonant frequency is reduced from mm wave to X band frequencies at down-state by using a meander type membrane, with the frequency band is being increased by adding two short high impedance lines at both ends of coplanar waveguide (CPW). Moreover, this acts as T-match circuit in up-state position and improves the matching. Simulation results demonstrate that the capacitance ratio reduces from 50 to 21.4, S_{21} and S_{11} are less than -10 dB for the entire frequency band at down-state and up-state. Also, a comprehensive and complete electric model of the switch is proposed and simulation results agree well with the characteristics of the physical structure of the MEMS switch. $V_{pull\text{-}in}$ and $V_{pull\text{-}out}$ of this switch are 8.1 V and 0.3 V, respectively.

Keywords: meander type beam, LC resonant frequency, discontinuity CPW, isolation, insertion loss

Classification: Micro- or nano-electromechanical systems

References

[1] G. Rebeiz, K. Entesari, I. Reines, S. J. Park, M. El-Tanani, A. Grichener and A. Brown: IEEE Microw. Mag. **10** [6] (2009) 55.

[2] M. Daneshmand and R. R. Mansour: IEEE Microw. Mag. **12** [5] (2011) 92.

[3] Y. Mafinejad, A. Z. Kouzani and K. Mafinezhad: Journal of Microelectronics, Electronic Components and Materials **43** (2013) 85.

[4] M. Zarghami, Y. Mafinejad, A. Z. Kouzani and K. Mafinezhad: IEICE Electron. Express **9** (2012) 1062.

[5] K. Topalli, M. Unlu, H. I. Atasoy, S. Demir, O. A. Civi and T. Akin: Prog. Electromagnetics Res. **97** (2009) 343.

[6] S. Lucyszyn: *Advanced RF MEMS* (Cambridge University Press, 2010) 23.

[7] R. N. Simons: *Coplanar Waveguide Circuits, Components, and Systems* (Wiley, New York, 2001) 11.

[8] Y. Mafinejad, A. Z. Kouzani, K. Mafinezhad and A. Golmakani: IEICE Electron. Express **6** (2009) 1483.

[9] K. Y. Chan, M. Daneshmand, R. R. Mansour and R. Ramer: Proc. SPIE

© IEICE 2013

DOI: 10.1587/elex.10.20130746
Received September 24, 2013
Accepted November 07, 2013
Publicized December 11, 2013
Copyedited December 25, 2013

6800, Device and Process Technologies for Microelectronics, MEMS, Photonics, and Nanotechnology **IV** (2008) 680026–1.

1 Introduction

The advancement of Micro and Nano electro mechanical systems (MEMS/NEMS) not only fabricate a new generation of electronic switches in micro or nano sizes but also meet the needs of future electronic industry by integration of MEMS switches and electronic devices on the same substrate. This reduces power consumption and size, increasing the linearity of the system and isolation [1, 2].

In our published comprehensive literature review paper we mentioned that there are two major drawbacks with capacitive RF MEMS switches [3]. The first major problem is the dielectric charging which we addressed this problem and proposed a novel ramp dual pulse (RDP) to reduce the actuation voltage shift and charging effect on the dielectric in our previous paper [4]. Another drawback of the capacitive MEMS switches is their isolation at low frequencies (X-Band) at down-state, depending on the LC ($f_{resonance}=1/2\pi(LC)^{-1/2}$) resonant behavior of the switch. Although, increasing the capacitor decreases the LC resonant frequency, this will require a large area. Therefore, MEMS switch should have a high capacitance ratio and this increases the actuation voltage [5].

In this paper we reduce the insertion loss and increase the isolation at C-K frequencies without increasing the ratio of capacitance. Moreover, we propose accurate electrical model to match with the physical structure.

Section two of this paper discusses the main parameters and the basics of RF MEMS switches. Section three focuses briefly on the design procedure, modelling and simulation results.

2 MEMS switch principle

2.1 Smith chart theory

The relation between match and unmatched condition can be found by S_{11} on the smith chart diagrams.

$$S_{11} - \frac{\Gamma}{1+\Gamma^2} = \frac{\Gamma}{1+\Gamma^2}\left(\frac{\Gamma^2 - e^{-2\beta l}}{1 - e^{-2\beta l}}\right). \tag{1}$$

$$\Gamma = \frac{Z_0 - Z_s}{Z_0 + Z_s}. \tag{2}$$

Where Γ is reflection coefficient, β is propagation constant, l is length of transmission line, Z_0 is characteristic impedance, Z_s is reference impedance. The S_{11} is always rotates clock wise around Z_0 from the dc point. The DC point is calculated from the input impedance of the transmission line.

$$Z_{in} = Z_0 \frac{Z_s + Z_0 tg(\beta l)}{Z_0 + Z_s tg(\beta l)}. \tag{3}$$

Therefore

© IEICE 2013
DOI: 10.1587/elex.10.20130746
Received September 24, 2013
Accepted November 07, 2013
Publicized December 11, 2013
Copyedited December 25, 2013

$Z_{0(f\to 0)} < Z_s$ then $Z_{0(f\to 0)} < Z_{in} < Z_s$, $Z_{0(f\to 0)} > Z_s$ then $Z_{0(f\to 0)} > Z_{in} > Z_s$

If $Z_0 < Z_s$, then S_{11} should rotate clock wise around Z_0 with the dc starting point between Z_0 and Z_s. Therefore, the circle is on the left side of the transmission line (Fig. 1 (a)). If $Z_0 > Z_s$, then S_{11} should rotate clock wise around Z_0 with the dc starting point between Z_0 and 50 Ω. Therefore, the circle is on the right side of the transmission line (Fig. 1 (a)). If $Z_0 = Z_s$, then the circle is at the center of the smith chart plane (Fig. 1 (a)), performing the ideal matching.

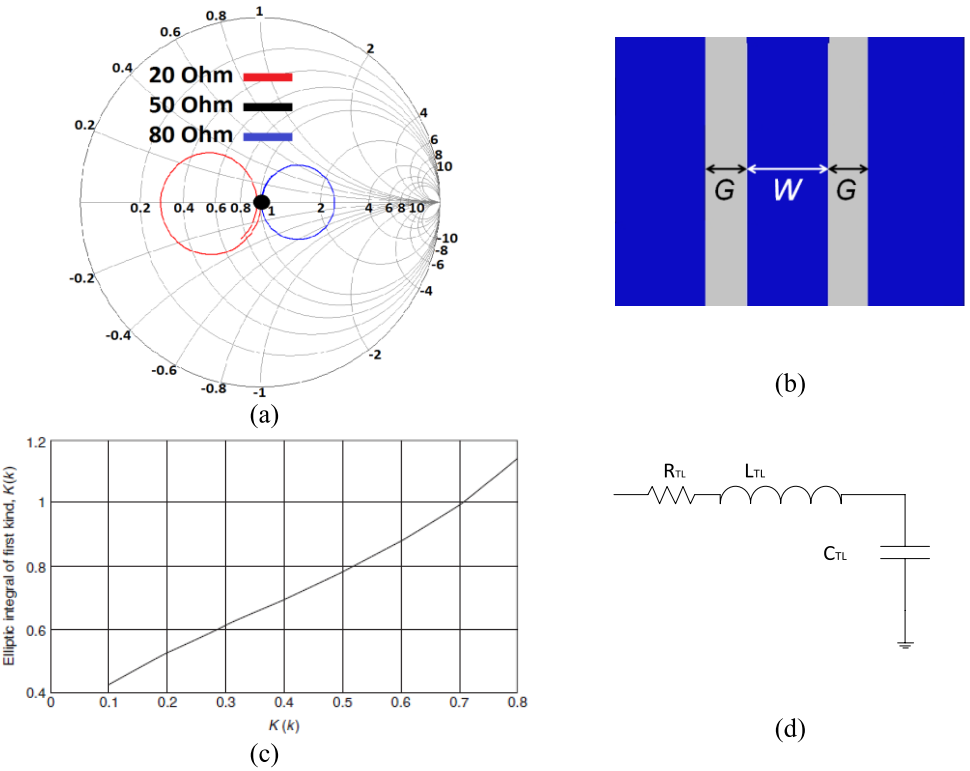

Fig. 1. (a) S_{11} for $Z_s = 50\,\Omega$ and $Z_0 = 80\,\Omega$, $50\,\Omega$ and $20\,\Omega$, (b) Normal $50\,\Omega$ CPW, signal line width (W=120 μm), the gap between signal line and ground (G=80 μm), (c) $K_{(k)}$ and $K_{(k')}$, (d) Electrical model of CPW transmission.

2.2 CPW transmission line

Coplanar waveguide (CPW) consists of one signal line in middle and two infinite grounds beside of transmission line (Fig. 1 (b)). The signal propagates between two identical slots and it has an inhomogeneous structure because the fields propagate within two media of dielectric and air.

2.2.1 Characteristic impedance

The effective substrate constant and characteristic impedance of transmission line are given in Eq. (4) and Eq. (5) [7].

$$e_{ff} = \left(\frac{e_r + 1}{2}\right)\left(\frac{0.5(e_r - 1)}{1 + 10(t/h)}\right). \tag{4}$$

© IEICE 2013
DOI: 10.1587/elex.10.20130746
Received September 24, 2013
Accepted November 07, 2013
Publicized December 11, 2013
Copyedited December 25, 2013

$$Z_{TL} = \left(\frac{94.25}{\sqrt{e_{ff}}}\right)\left(\frac{K_{k'}}{K_k}\right). \tag{5}$$

Where e_r is a relative constant substrate, t and h are a conductor thickness and a substrate height, respectively.

$$k = \frac{W}{W + 2G}. \tag{6}$$

$$k' = \sqrt{1 - k^2}. \tag{7}$$

Where W is the signal conductor width, G is the gap between center conductor and ground. $K_{(k)}$ and $K_{(k')}$ can be calculated from Fig. 1 (c).

2.2.2 Electrical model

The electrical model of CPW is shown in Fig. 1 (d), where L_{TL}, C_{TL} are the intrinsic inductance and capacitance, depending on the impedance of TL. The loss is represented by the R_{TL}. R_{TL} is related to the loss of CPW transmission, relating to the loss of substrate penetration and loss of metal.

The first type is due to the propagation of electric field inside the CPW and generating an induced current which is in orthogonal direction of the wave propagation. This loss can be ignored for high resistivity substrates. The second type of loss, affecting on the loss of the CPW is the resistivity of material due to the effect of skin depth on transmission line, because the resistance of material is increased at higher frequency [8]. The loss of metal can be ignored if the thickness of Au is more than 1.5 μm.

$$L_{TL} = \frac{\sqrt{e_{ff}} Z_0}{c}. \tag{8}$$

$$C_{TL} = \frac{L_{TL}}{{Z_0}^2}. \tag{9}$$

Where c is the speed of light (3×10^8 m/s).

2.3 Electrical and mechanical model of MEMS switch

2.3.1 Electrical model

The electrical model of MEMS switch is shown in Fig. 2 (a). The operation of MEMS switch strongly depends on the frequency and approximated by Eq. (10) [6, 8]. The CLR model behaves as a capacitor below the resonant frequency, as a resistor at resonant frequency and inductor above this frequency.

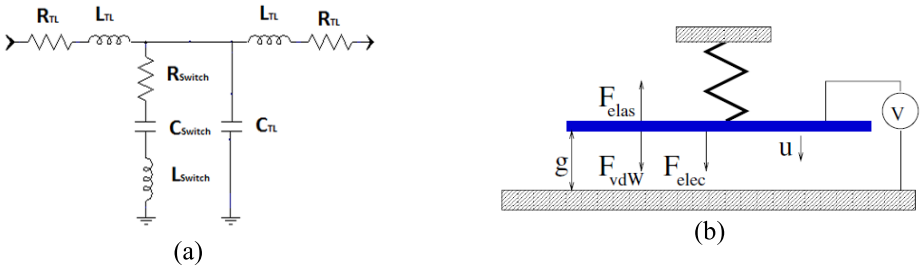

Fig. 2. (a) Electrical model, (b) Mechanical model.

© IEICE 2013
DOI: 10.1587/elex.10.20130746
Received September 24, 2013
Accepted November 07, 2013
Publicized December 11, 2013
Copyedited December 25, 2013

$$Z_s = \begin{cases} \dfrac{1}{j\omega C} & \omega << \omega_0 \\ R_s & \omega = \omega_0 \\ j\omega L & \omega >> \omega_0 \end{cases} . \quad (10)$$

$$\omega_0 = \frac{1}{\sqrt{LC}}$$

2.3.2 Mechanical model

The mechanical model of the MEMS switches is shown in Fig. 2 (b). Increasing the actuation voltage ($V_{pull\text{-}in}$) makes instability and causes the upper electrode to snap down at $V_{pull\text{-}in}$. The membrane still in down-state until $V_{pull\text{-}out}$ due to the wan deer Waals force and the upper electrode is released at the hold down voltage because of the elastic force (Eq. (11) and Eq. (12)).

$$V_{pull\text{-}in} = \sqrt{\frac{8k_{switch}}{27\varepsilon_0 W w} g_0^3}. \quad (11)$$

$$V_{pull\text{-}out} = \sqrt{\frac{2k_{switch}}{\varepsilon\varepsilon_0 W w}(g_0 - g)\left(g + \frac{t_d}{\varepsilon_r}\right)^2}. \quad (12)$$

Where k_{switch}, g_0, t_d, A are the spring constant, gap between transmission line and bridge, dielectric thickness and overlap area between transmission line and the bridge.

3 Design and simulation

According to previous section the isolation of the switch at down-state depends on the LC resonant behavior of the switch. The analysis based on the lumped model of MEMS switch shows that increasing the inductance of the MEMS bridge reduces the LC resonant frequency, improving the isolation at lower frequency but it narrows the frequency band. Fig. 3 (a) compares three types of MEMS Switches: normal switch, switch with inductive arm and switch with both inductive arm and inductive TL- at down-state position. It is seen that the LC resonant frequency of normal switch is at mm-wave frequency; also the low frequency is at 10 GHz. The resonant frequency and the lower frequency for the other two types of switch are same and irrespective from the TL (5 GHz and 8 GHz, respectively), but the upper frequency for switch with both inductive arm and transmission line is higher than the inductive arm (25 GHz and 15 GHz, respectively).

The proposed MEMS switch physical structure is shown in Fig. 3 (b). It consists of meander type beam and discontinuity transmission line CPW (Fig. 3 (c and d)).

3.1 Inductive beam design

The membrane of the switch is a low spring constant dual beam (Fig. 3 (c)). The dimensions of the beam are given in Table I. The spring constant of a structure with N numbers of L-shaped meanders is given in (Eq. (13–16)) [9]

© IEICE 2013
DOI: 10.1587/elex.10.20130746
Received September 24, 2013
Accepted November 07, 2013
Publicized December 11, 2013
Copyedited December 25, 2013

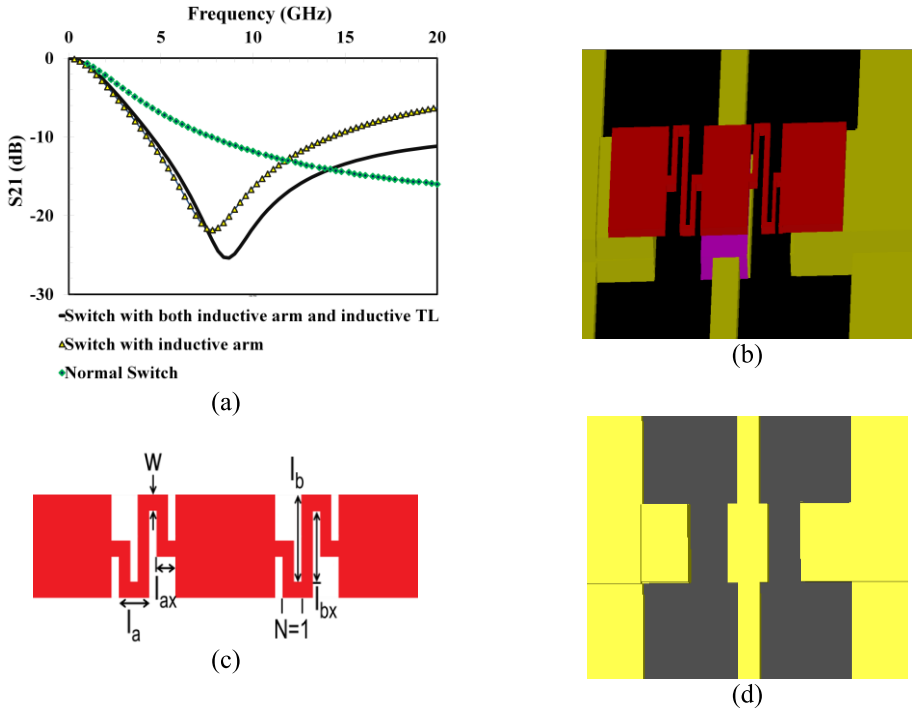

Fig. 3. (a) Comparing the electrical model of MEMS switch at down-state by Genesys, (b) proposed RF MEMS switch, (c) Meander type membrane, (d) Discontinuity transmission line CPW.

Table I. Physical structure of RF MEMS switch.

Parameter	Value	Parameter	Value
Membrane width (w)	140μm	Dielectric thickness	1000 Å
Membrane length (L)	280μm	Gap between TL and membrane (g_0)	2.5μm
Signal line width (W)	120μm	Bridge thickness	1.5μm
Gap between signal line and ground (G)	80μm	HR silicon Substrate constant (ε)	11.6
Overlap area	120×140μm^2	Fringing constant (k)	1.4
CPW thickness	2μm		

$$k_{meander} = \left[N k^{-1}_{fixed\text{-}guided}\big|_{l=l_{bx}} + 2k^{-1}_{fixed\text{-}guided}\big|_{l=l_{bx}/2} \right]^{-1}. \quad (13)$$

Where, $k_{fixed\text{-}guided}$ is the spring constant of the beam that can be calculated as follow

$$k_{fixed\text{-}guided} = w_m E \left(\frac{t}{l}\right)^3. \quad (14)$$

Where, w_m is the width of the beam, E is the Young's Modulus, t is the thickness of the beam, l is the length of the beam. Finally, Eq. (15) can be used to calculate the spring constant of the switch as follows

$$k_{switch} = \left(k^{-1}_{meander} + k^{-1}_{beam} + k^{-1}_{meander}\right)^{-1}. \quad (15)$$

If $k_{beam} \gg k_{meander}$, Eq. (15) reduces to

$$k_{switch} = k_{meander}/2. \quad (16)$$

With the meander geometry $l_a = 45\,\mu m$, $l_b = 120\,\mu m$, $w_m = 20\,\mu m$, $t = 1.5\,\mu m$, and A (actuation area) $= 120 \times 140\,\mu m^2$. Thus, calculated spring

© IEICE 2013
DOI: 10.1587/elex.10.20130746
Received September 24, 2013
Accepted November 07, 2013
Publicized December 11, 2013
Copyedited December 25, 2013

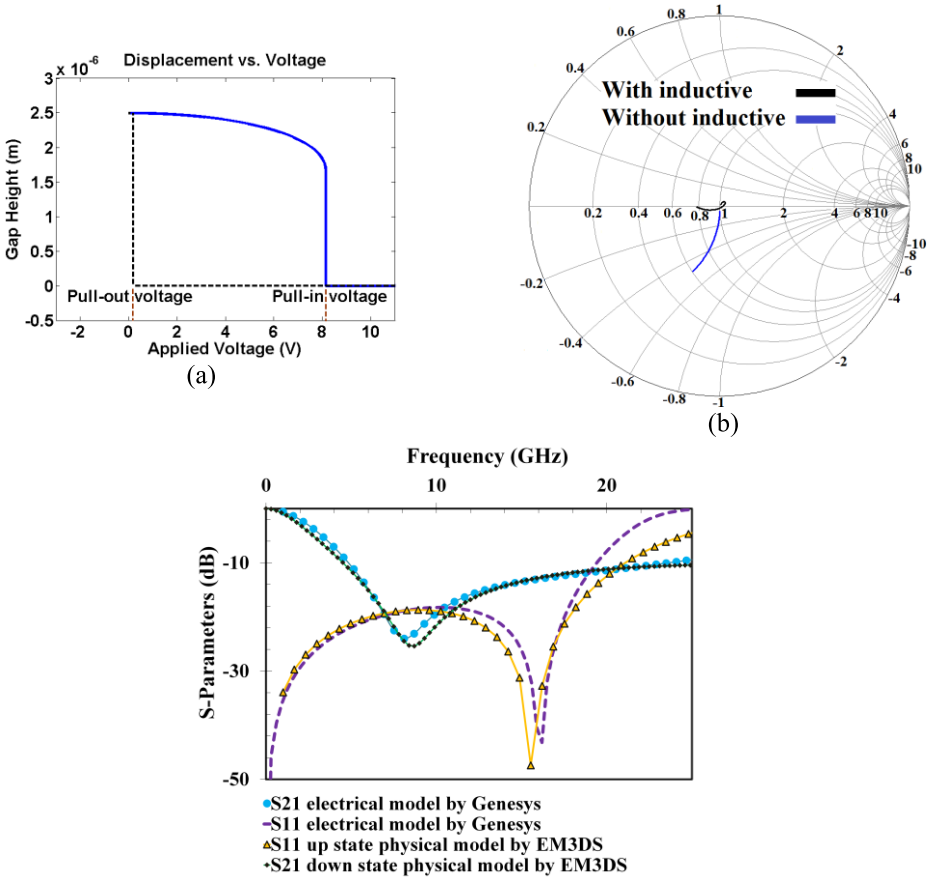

Fig. 4. (a) $V_{pull\text{-}in}$ and $V_{pull\text{-}out}$, (b) Comparison the switch with and without inductor at up-state, (c) Comparing the S_{11} and S_{21} for the up and down states for both physical structure and electrical lumped model with EM3DS and Genesys2012.01.

constant, $V_{pull\text{-}in}$ and $V_{pull\text{-}out}$ are 2.1N/m, 8.1 V and 0.3 V, respectively (Fig. 4 (a)).

The switch at down-state should provide a good isolation between input and output (S_{21}<−10 dB). The TL consists of 50 Ω for overlapping area and two high impedance TLs (90 Ω) with the length of 230 μm in order to increase the inductance of the switch (2 nH). According to our simulation with EM3DS the inductance of the bridge is 115 pH, which assures a good isolation at down-state.

The amount of capacitance at up-state should provide a good matching between input and output of the switch Z_{in}=Z_0. The input impedance for the above switch is given in Eq. (17).

$$Z_{in} = \left[(Z_0 + R_{TL} + j\omega L_{TL}) || \frac{1}{j\omega C_{TL}} || \left(\frac{1}{j\omega C_{switch}} + R_{switch} + j\omega L_{switch} \right) \right] + R_{TL} + j\omega L_{TL}. \quad (17)$$

According to the frequency operation the C_{TL}, R_{TL}, R_{switch} can be ignored in Eq. (17) and therefore,

$$Z_{in} = (Z_0 + j\omega L_{TL}) || \left(\frac{1}{j\omega C_{switch}} + j\omega L_{switch} \right) + j\omega L_{TL}. \quad (18)$$

© IEICE 2013
DOI: 10.1587/elex.10.20130746
Received September 24, 2013
Accepted November 07, 2013
Publicized December 11, 2013
Copyedited December 25, 2013

For $Z_{in} = Z_0$, $C_{up\text{-}state} \sim 0.1$ pF and therefore the gap between TL and bridge should be 2.5 μm. The comparison of the switch with and without inductive transmission line (SHITL) is shown in Fig. 4 (b), the addition of SHITL gathers the values of passband S_{11} closer to the center of the Smith chart, leading to wideband matching between input and output.

3.2 Electrical model and simulation result of MEMS switch

The scattering parameters are shown in Fig. 4 (c). At down-state position the inductive arm reduces the LC resonant from mm-wave to X band (8 GHz) and S_{21} is less than -10 dB at 20 GHz. The RF parameters of the switch are improved by adding two SHITLs at up state. It is seen the S_{11} is less than -15 dB for the frequency up to 20 GHz. Furthermore, there is desirable matching at 15 GHz for S_{11} less than -45 dB.

The electrical lumped model of the switch is shown in Fig. 2 (a) and the values of parameters are given in Table II. It can be seen there is an outstanding matching between the electrical model and physical structure.

Table II. Electrical model of RF MEMS switch.

Parameter	Value	Parameter	Value
$C_{switch(up)}$	0.1pF	R_{switch}	0.2Ω
$C_{switch(down)}$	2.5pF	L_{TL}	0.23nH
L_{switch}	115pH	C_{TL}	0.02pF

4 Conclusion

Although the RF performance of any RF MEMS shunt capacitive switch can be improved by increasing the ratio of its capacitance ($C_{ratio} = C_{Down}/C_{up}$), this will increase the actuation voltage. This paper shows how to improve the RF performance without increasing the capacitance ratio. The inductance of the MEMS switch is increased from 5 to 115 pH by using a proper meander supporting bridge between the signal line and the ground. This reduces the LC resonance from the mm-wave into the X-band, increasing the isolation and narrowing the bandwidth at down-state. In order to increase the bandwidth at down-state, we use two short high impedance transmission lines at both ends of the CPW. This improves the matching between the switch and I/O ports at C-K band, the matching at the entire frequency band at the up-state by cancelling the capacitive behavior of the switch. This method decreases the capacitance ratio from 50 to 21 and the switch can be used for the C-K band.

© IEICE 2013
DOI: 10.1587/elex.10.20130746
Received September 24, 2013
Accepted November 07, 2013
Publicized December 11, 2013
Copyedited December 25, 2013